Ionoacoustic Bragg Peak Localization for Charged Particle Cancer Therapy

Siavash Yousefi, December-9-2015

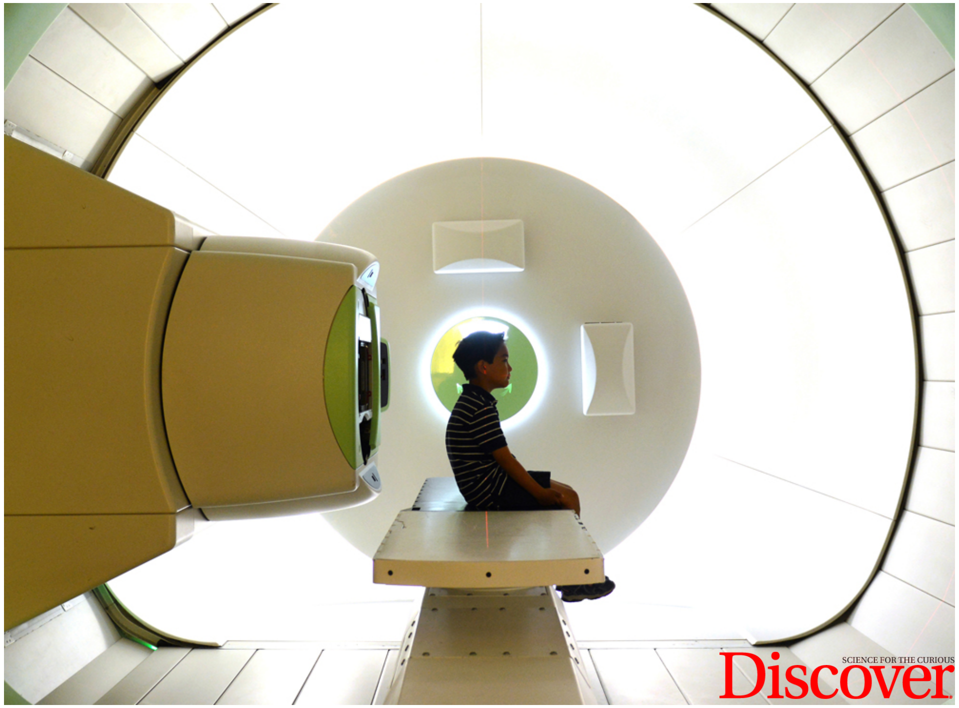

Jonathan Alava, 7
Roberts Proton Therapy Center in Philadelphia

Cancer Treatment: Protons vs. X-ray

Superior Dose Distribution

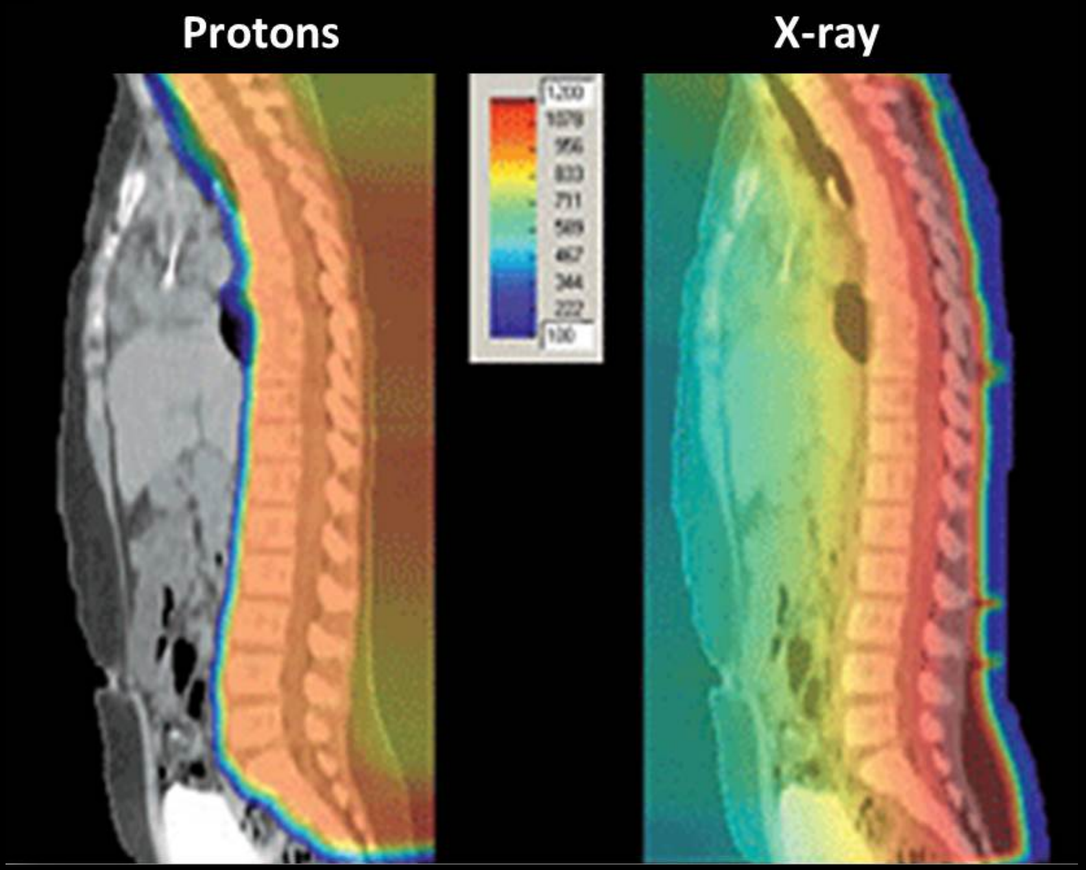

Photon vs. Proton Dose Distribution

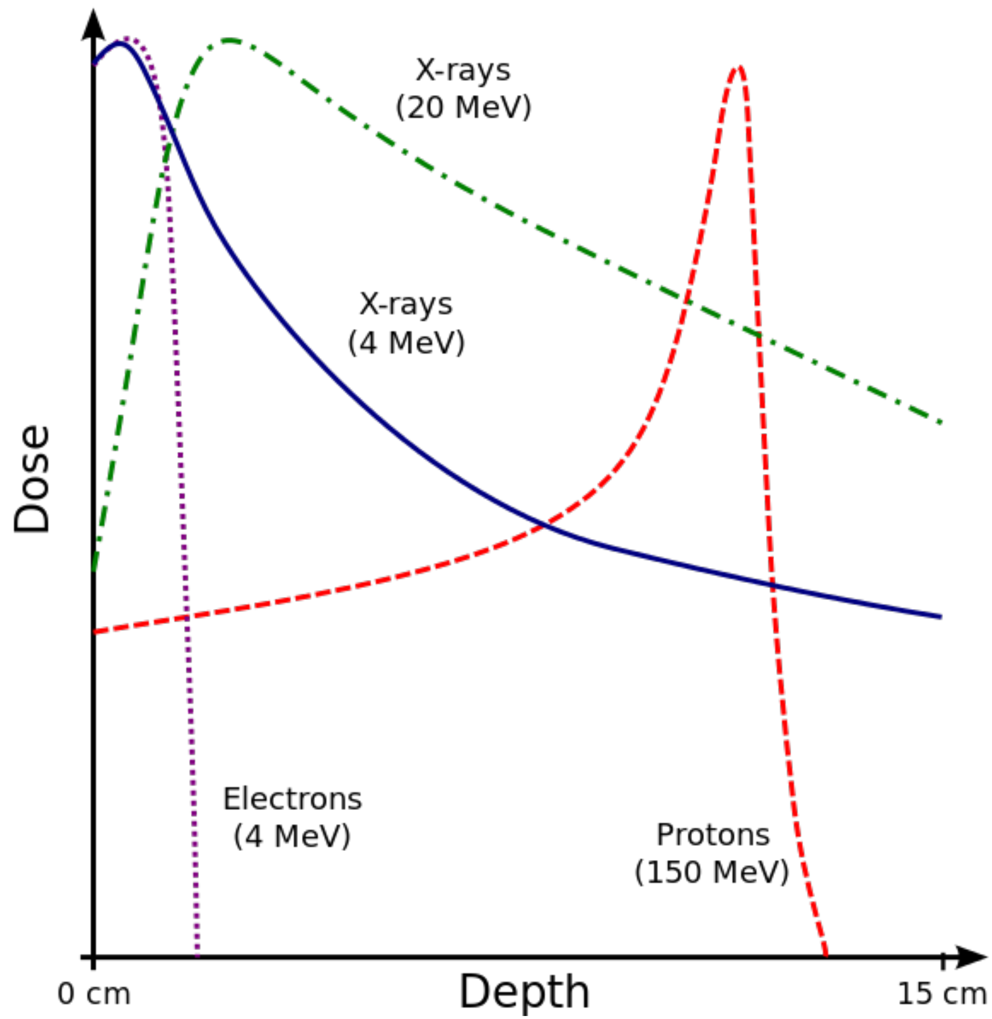

http://www.wikiwand.com/en/Particle_therapy

Proton and Carbon Therapy Facilities

Carbon Therapy Facilities

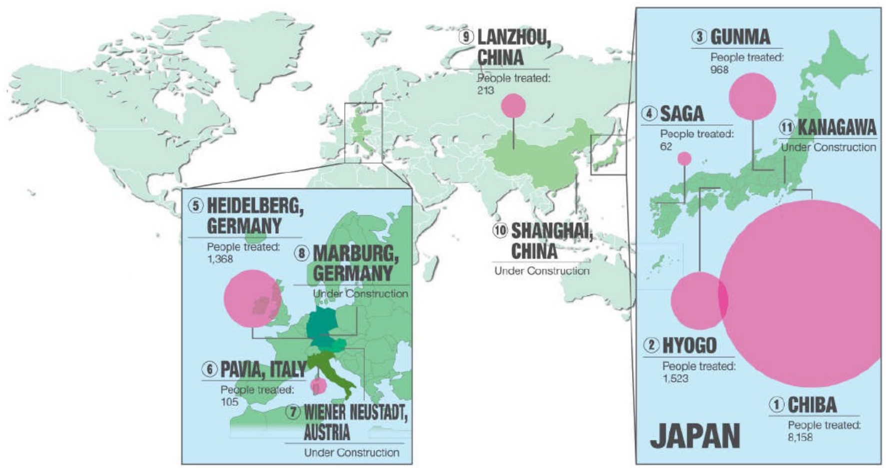

MITSUBISHI ELECTRIC
Changes for the Better

PROTON THERAPY FACILITIES

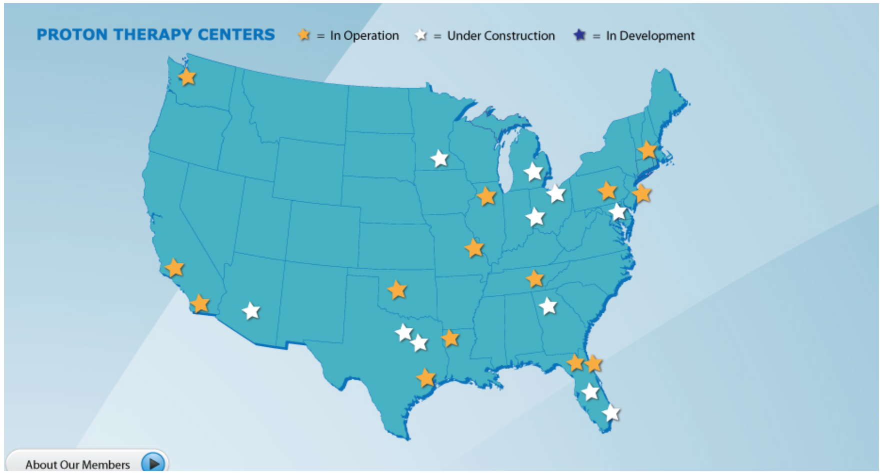

The National Association for Proton Therapy

External Beam LINAC

VARIAN
medical systems

External Beam LINAC

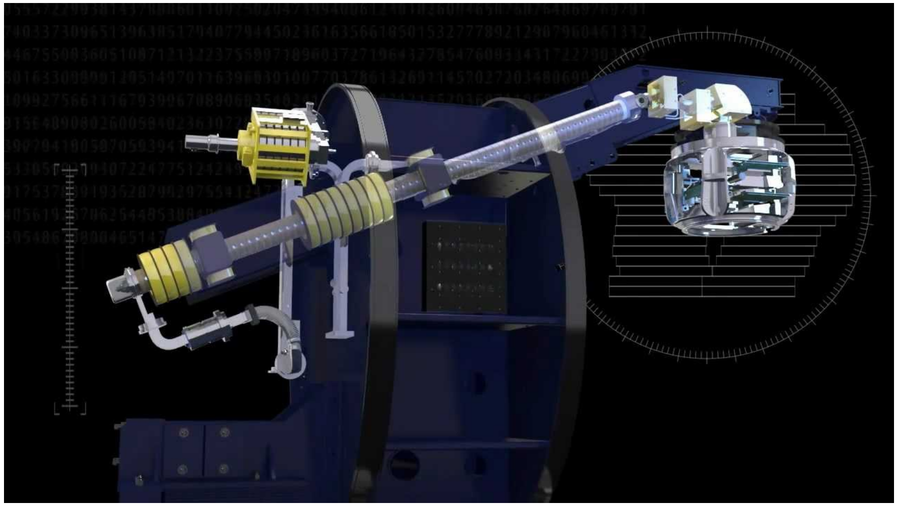

Proton Therapy Facility

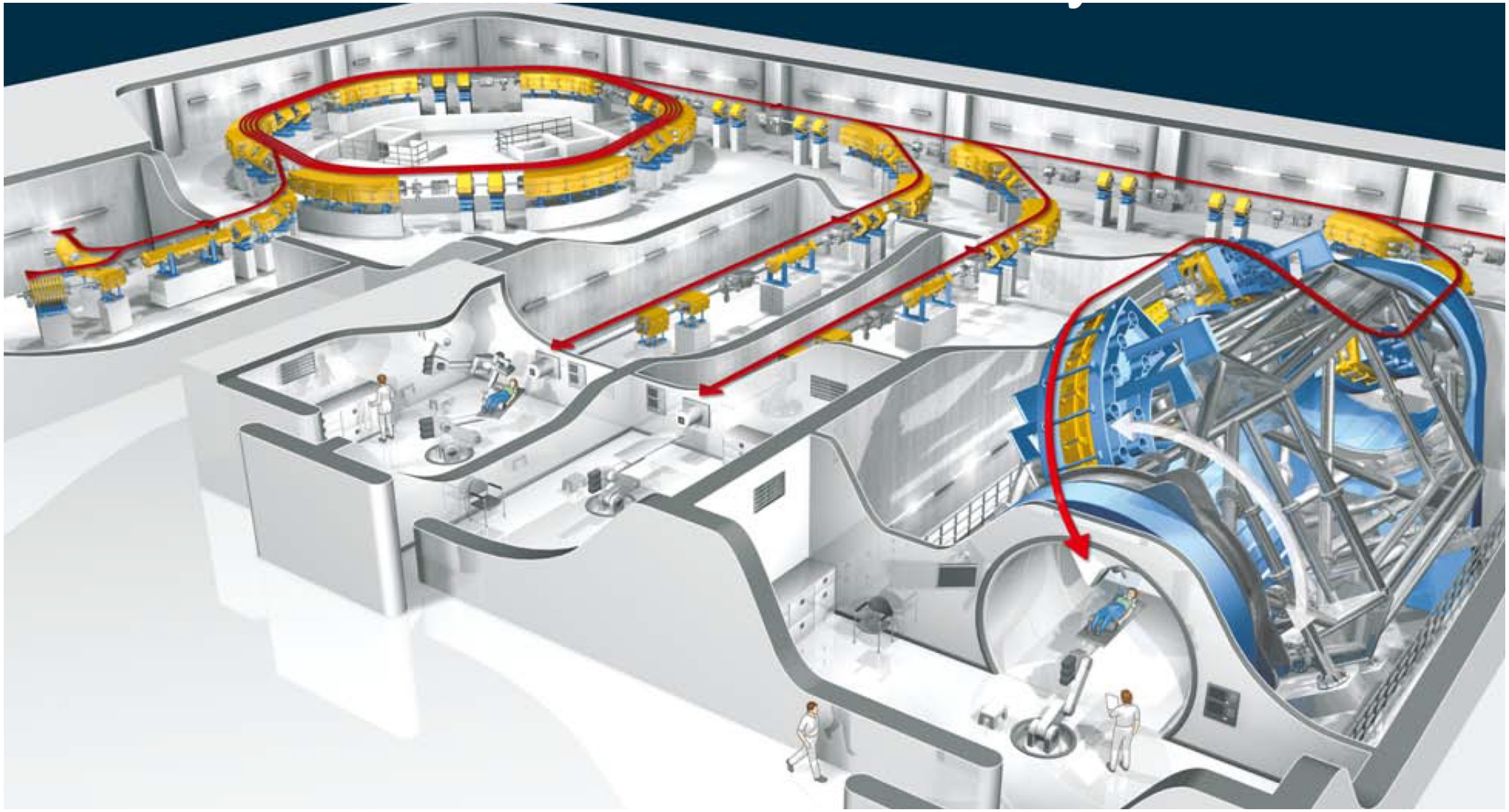

Heidelberg Ion Therapy Center

60m x 70m Compact Design

Uncertainties in Proton Therapy

- Due to sharp dose fall-off at Bragg peak
- Protons are more sensitive to uncertainties than photon
- Damaging surrounding healthy tissue/not treating tumor

Sources of uncertainties

- Stochastic error (CT noise)
- CT artifacts
- CT resolution (partial volume effect)
- Hounsfield unit (HU) conversion method

Proton Range Verification Techniques

Measurement technique

- *Direct*
- *Indirect*: range is implied from another signal

Timing

- *Online:* during treatment delivery
- *Offline:* performed after completion of the treatment

	Direct	**Indirect**
Online	Range probes Proton radiography	Prompt gamma imaging (3D) PET imaging (3D) **Ionoacoustic**
Offline		PET imaging (3D) MRI (3D)

PET Imaging for Range Verification

- Protons and heavy ions cause nuclear fragmentation reactions
- Generation of positron emitting isotopes (^{15}O, ^{11}C)
- PET scan measures the distribution of activities
- Clinically appealing; no additional dose to the patient

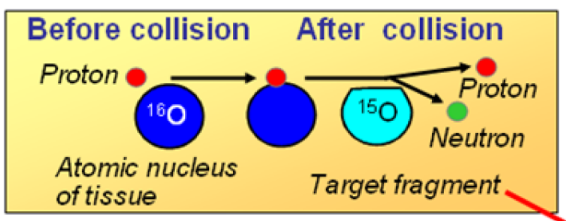

Mainly ^{11}C ($T_{1/2}$ = 20.3 min) and ^{15}O ($T_{1/2}$ = 121.8 s)

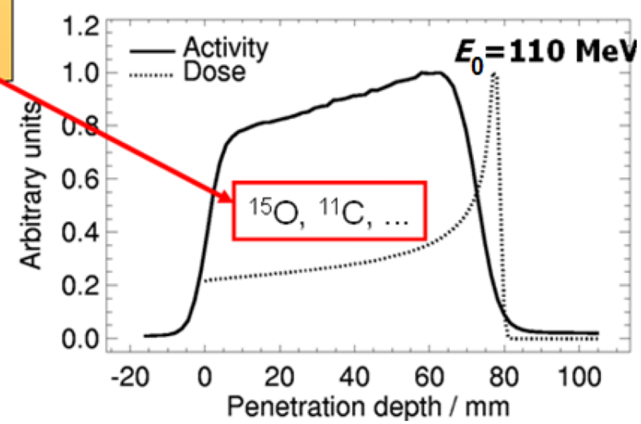

Dose proportionality:

$A(\mathbf{r}) \neq D(\mathbf{r})$

PET Verification of Proton Therapy:
Operational Modalities

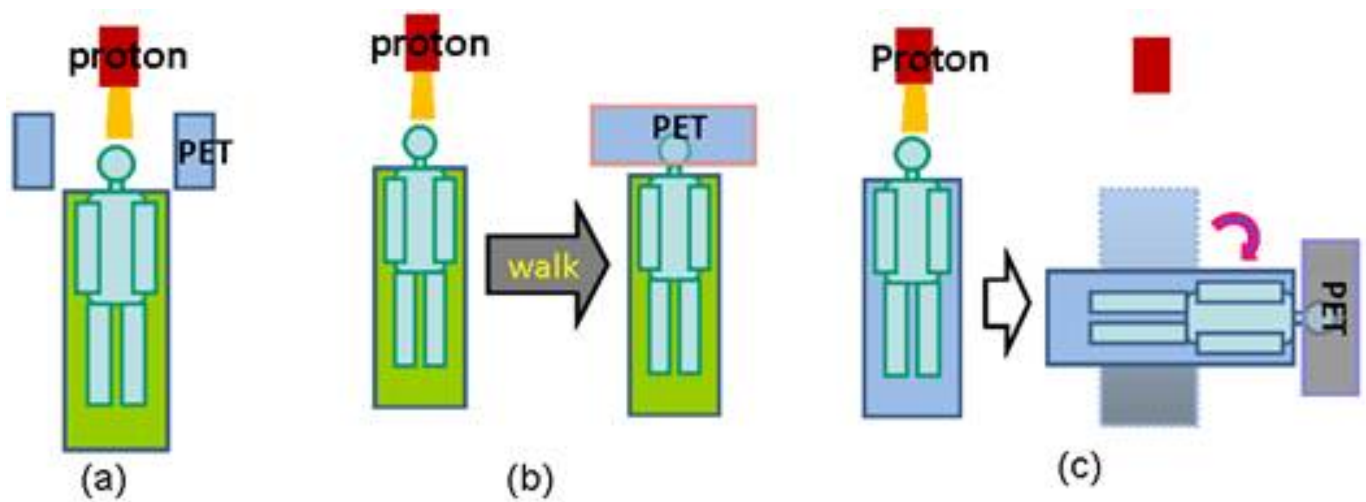

In-beam PET   Offline PET   In-room PET

PET Verification Studies in Patient

Clival chordoma receiving a posterior–anterior followed by a lateral field

~26 min (T_1) and 16 min (T_2) after completion.

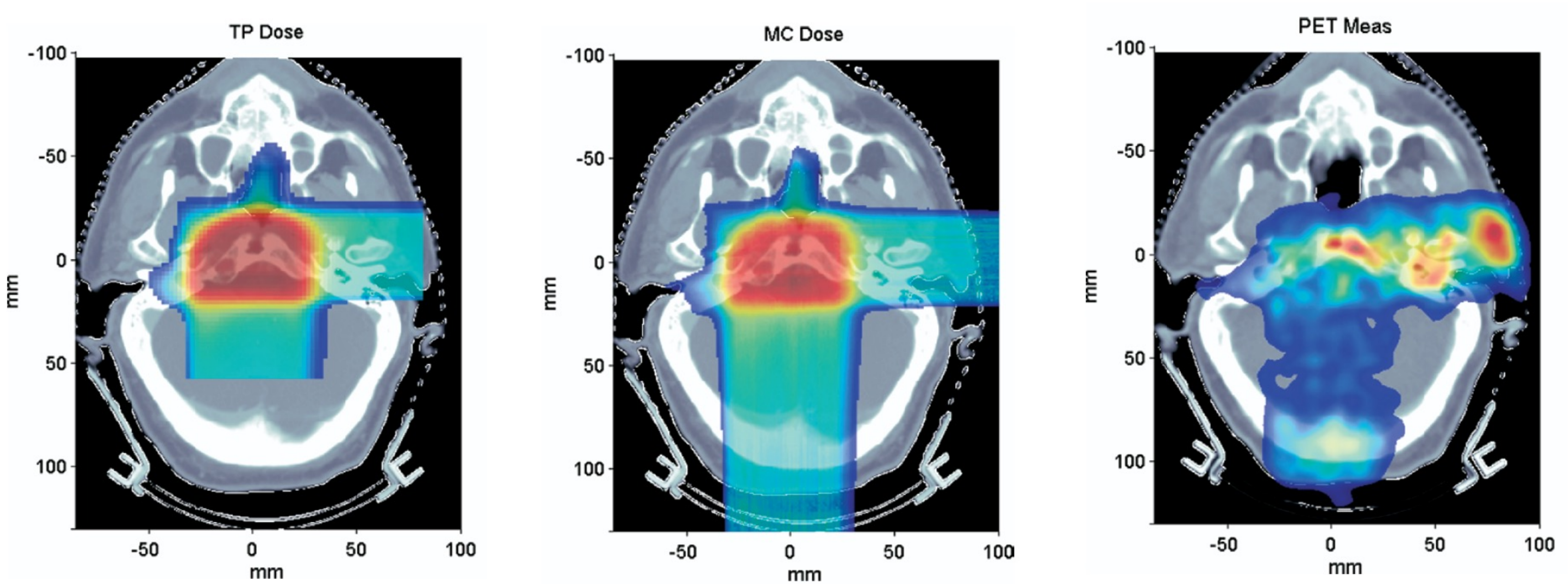

Parodi, Katia, et al. "Patient study of in vivo verification of beam delivery and range, using positron emission tomography and computed tomography imaging after proton therapy." *International Journal of Radiation Oncology* Biology* Physics* 68.3 (2007): 920-934.

ELSEVIER

(Offline) PET Disadvantages

- Long delay for PET acquisition (~15-30 min)
- Can only measure contributions from long half-life (^{11}C)
- Performance is degraded by biological washout of the proton-induced PET
  - Specially for tissues with high perfusion rates
- Repositioning errors and patient anatomical changes during the transportation and reposition

Ionoacoustic Characterization of the Bragg Peak (1979)

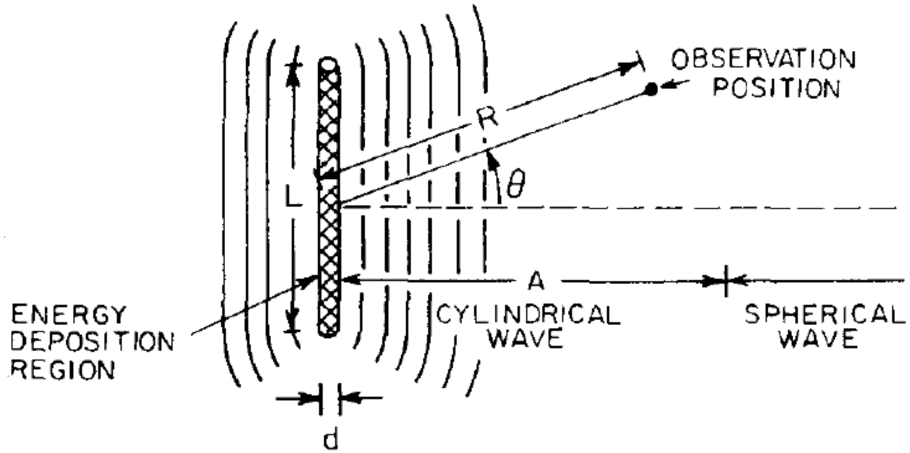

Acoustic radiation from idealized cylindrical energy deposition

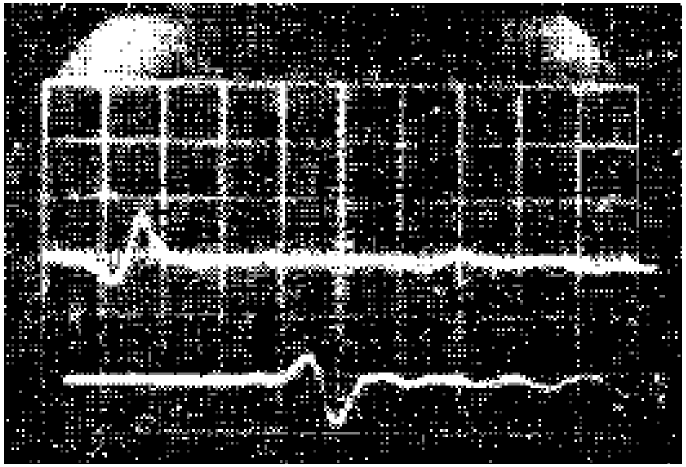

Typical signals from the hydrophones

Sulak, L., et al. "Experimental studies of the acoustic signature of proton beams traversing fluid media." *Nuclear Instruments and Methods* 161.2 (1979): 203-217.

Ionoacoustic Characterization of the Bragg Peak (1991)

Experimental Set up

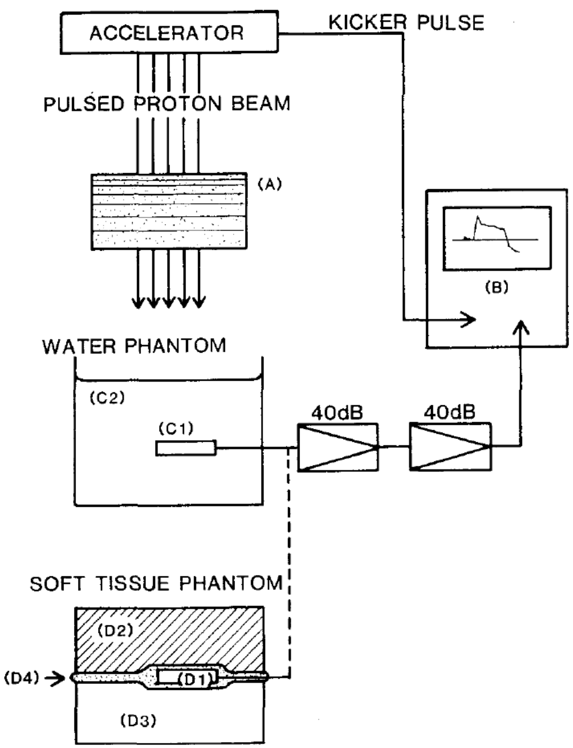

Acoustic pulses and corresponding depth dose distribution
Range: 51 and 81 mm in water

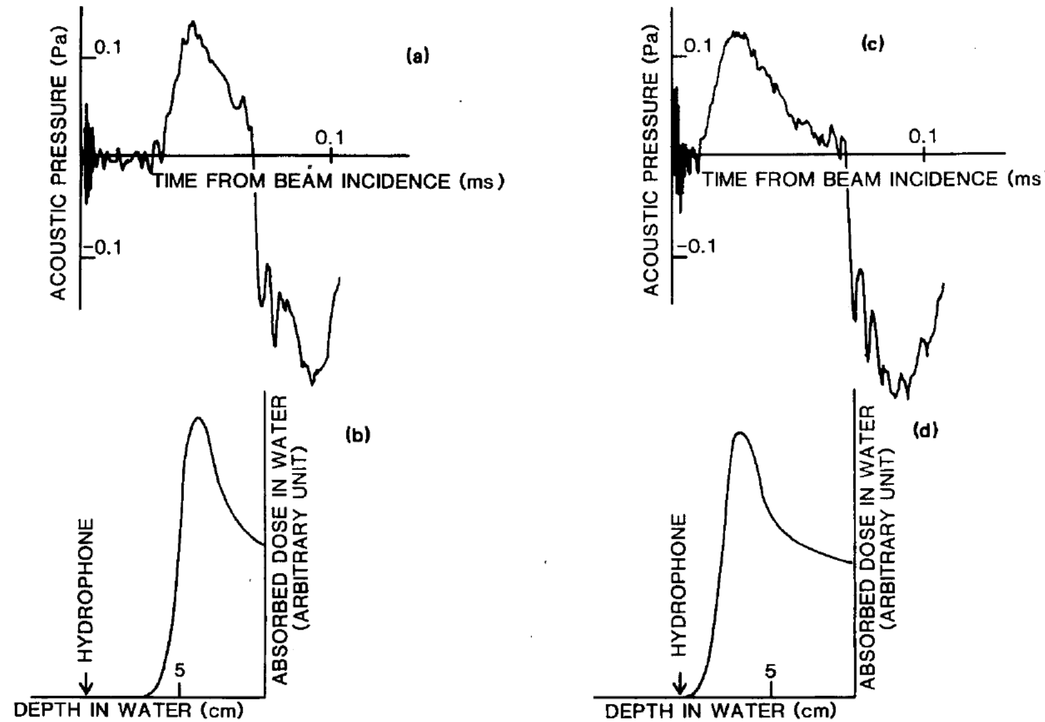

Tada, JunIchiro, et al. "Time resolved properties of acoustic pulses generated in water and in soft tissue by pulsed proton beam irradiation—A possibility of doses distribution monitoring in proton radiation therapy." *Medical physics* 18.6 (1991): 1100-1104.

Ionoacoustic Characterization of the Bragg Peak (1995)

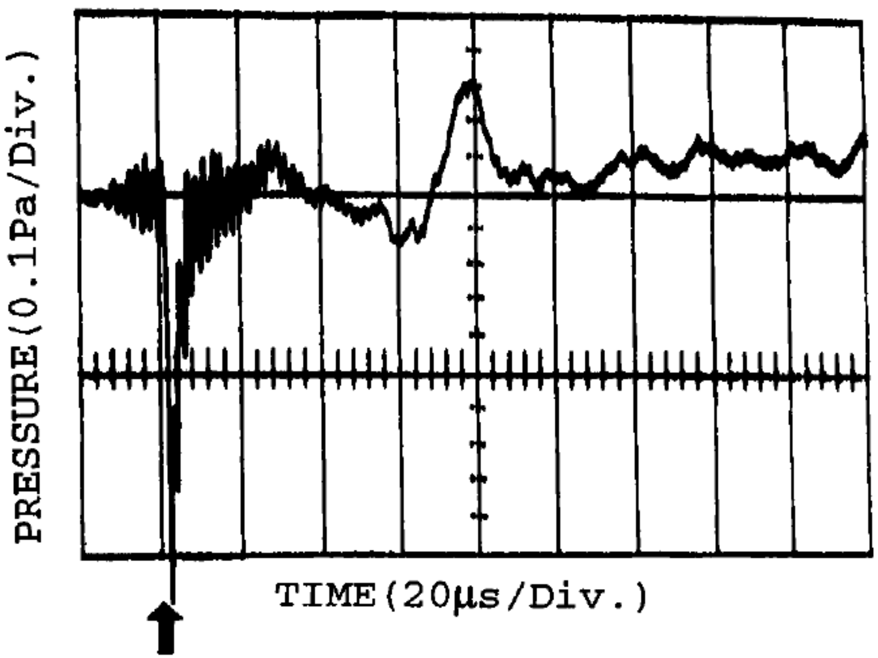

Acoustic pulse measured with a hydrophone

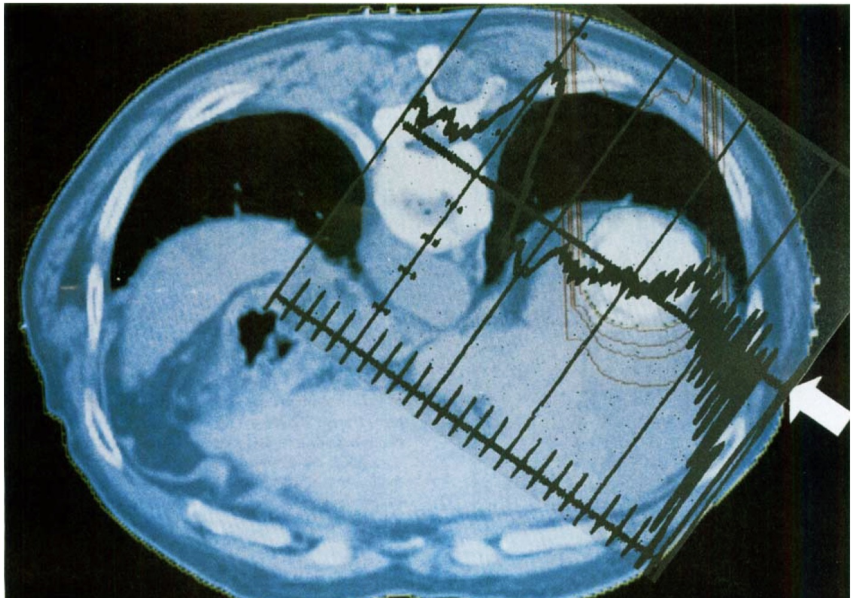

Treatment plan (hepatic cancer patient)

Hayakawa, Yoshinori, et al. "Acoustic pulse generated in a patient during treatment by pulsed proton radiation beam." *Radiation Oncology Investigations*3.1 (1995): 42-45.

Ionoacoustic Characterization of the Bragg Peak (2015)

Experimental Set up

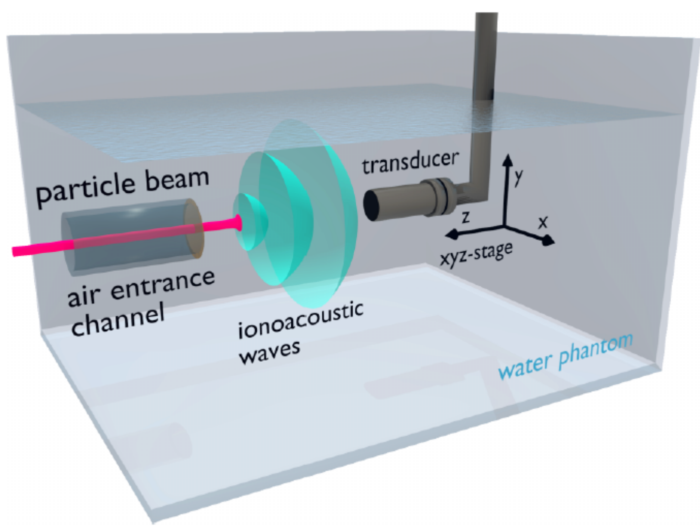

Measured acoustic signal

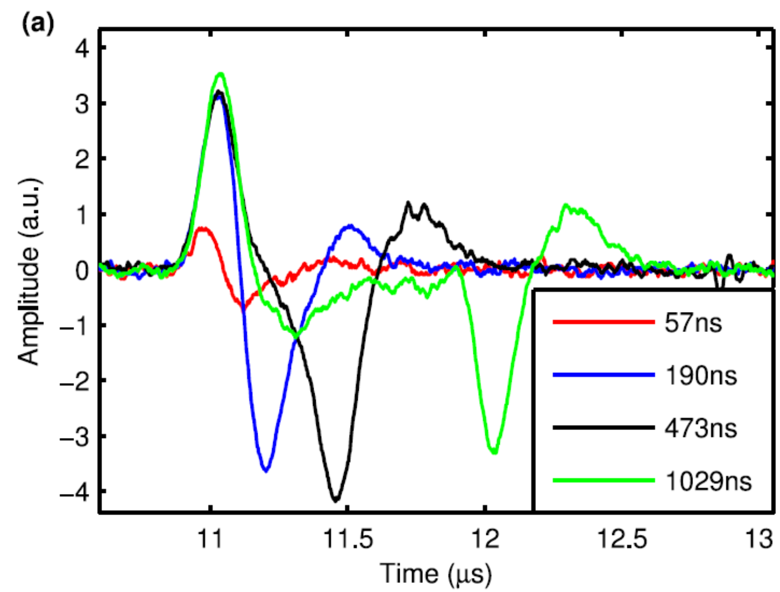

$$\left(\nabla^2 - \frac{1}{v_s^2}\frac{\partial^2}{\partial t^2}\right) p(r,t) = -\frac{\beta}{\kappa v_S^2}\frac{\partial^2 T(r,t)}{\partial t^2}$$

Assmann, W., et al. "Ionoacoustic characterization of the proton Bragg peak with submillimeter accuracy." *Medical Physics* 42.2 (2015): 567-574.

Photoacoustic Imaging

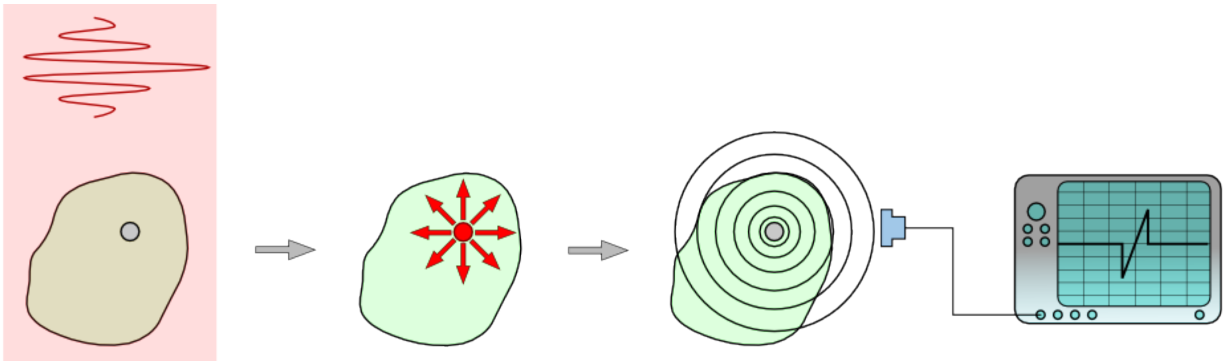

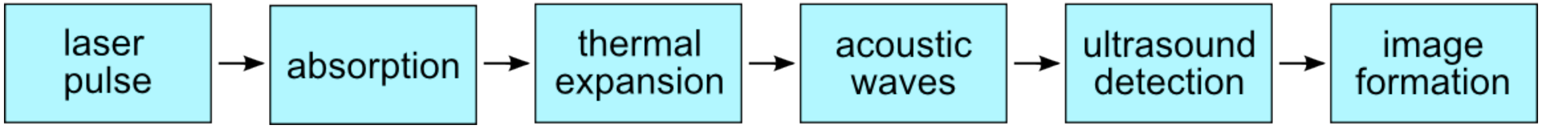

$$(\nabla^2 - \frac{1}{v_S^2}\frac{\partial^2}{\partial t^2})\, p(r,t) = -\frac{\beta}{\kappa v_S^2}\frac{\partial^2 T(r,t)}{\partial t^2}$$

$$t_L < \frac{d_c}{v_S} < \frac{d_c^2}{4\alpha_{th}}$$

Acoustic confinement

Thermal confinement

Quantifying Propagating of Acoustic Waves

Energy Deposition

- Ionizing radiation
- Pulsed laser
- High-energy acoustic

Acoustic Waves

- Propagating waves
- Shear Waves
- N-wave
- Shockwaves

Measurement (Imaging)

- Passive Detection
- Motion Detection
- High-frame rate imaging

Simulation Studies

Dose distribution 160 MeV beam
10-μs pulse width, 647 mGy/pulse

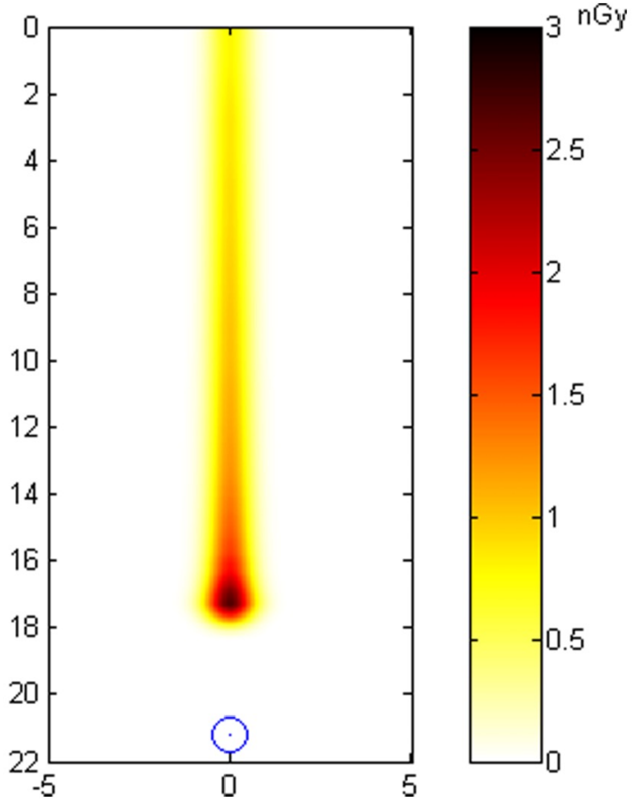

Simulated acoustic waveforms
Detector at 4 cm from the Bragg peak

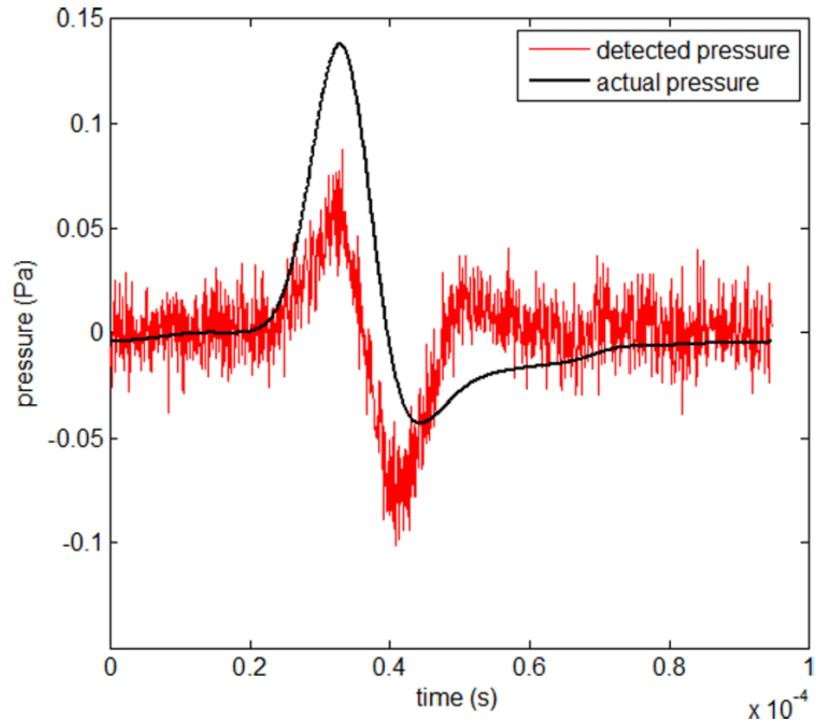

Ahmad, M., Xiang, L., Yousefi, S., & Xing, L. (2015). Theoretical detection threshold of the proton-acoustic range verification technique. *Medical physics*, *42*(10), 5735-5744.

Simulation Studies

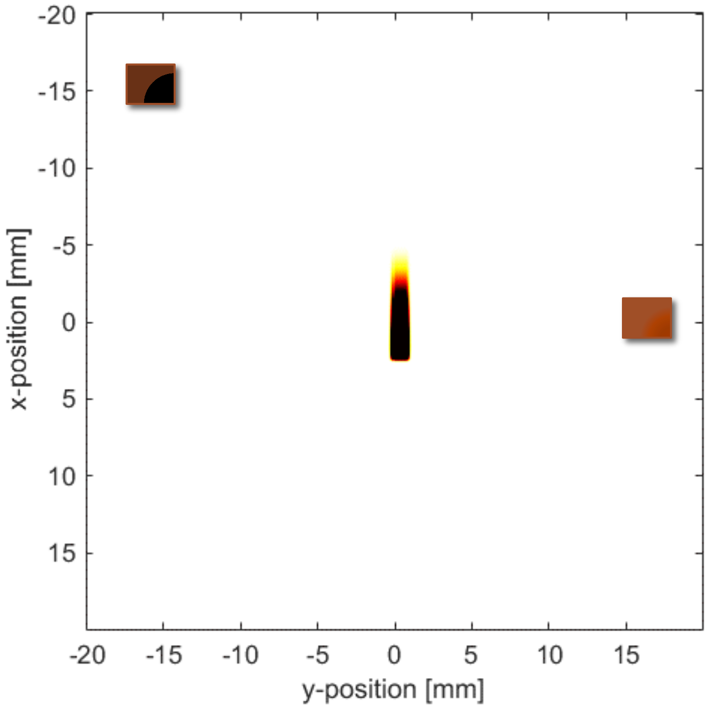

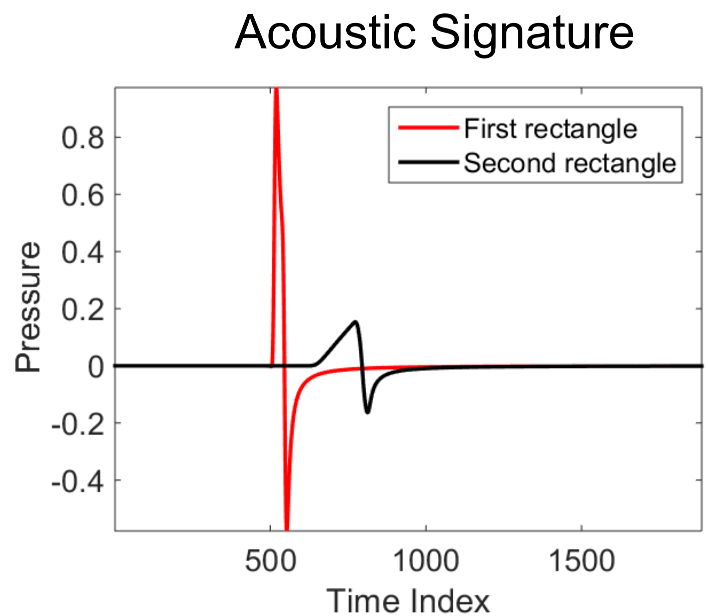

$$\left(\nabla^2 - \frac{1}{v_s^2}\frac{\partial^2}{\partial t^2}\right) p(r,t) = -\frac{\beta}{\kappa} v_S^2 \frac{\partial^2 T(r,t)}{\partial t^2}$$

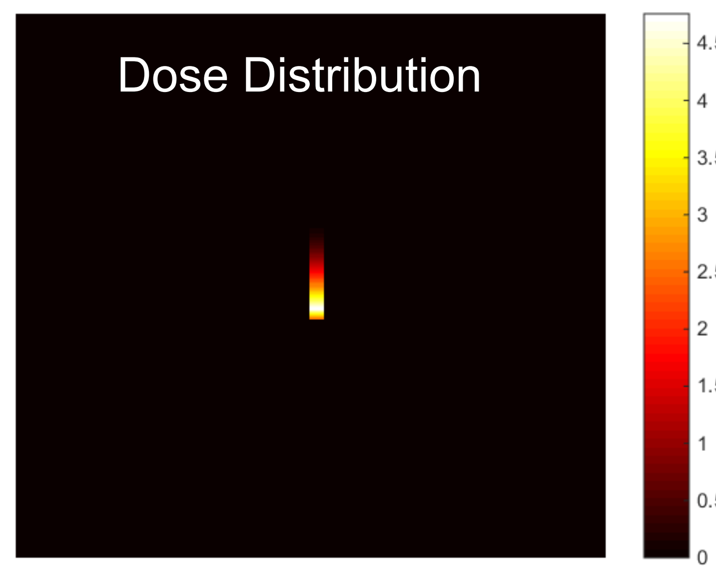

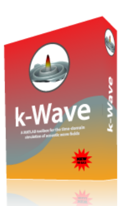

Passive Ionoacoustic Disadvantages

- Only measuring compressional waves
- Not considering tissue scattering/attenuation
- Experimental settings are very extreme
- Requires averaging multiple pulse signals
- Transducer placement
- Matching the with exact anatomical structures
- **Really sub-millimeter?!**

OCT Imaging of Laser-Generated Wave Propagation

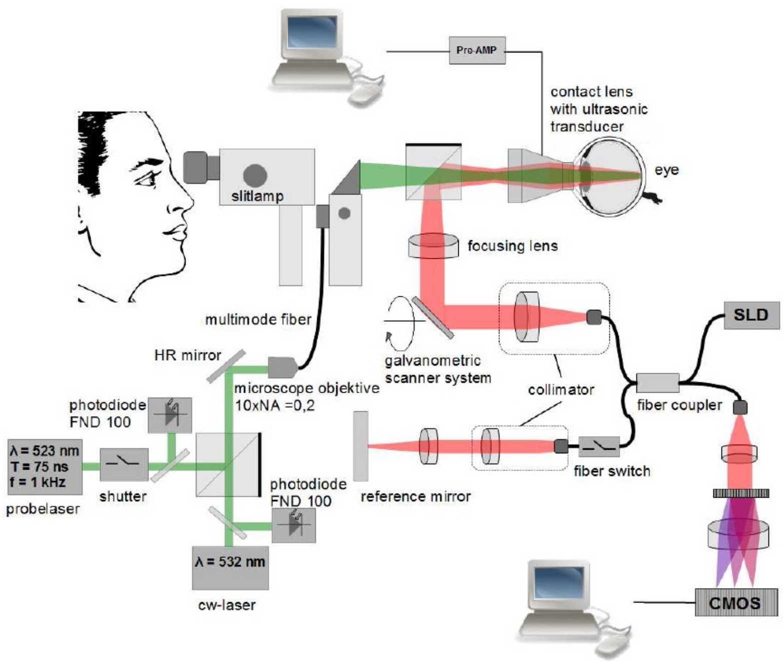

532 nm CW coagulation laser + OCT for visualization of the retina

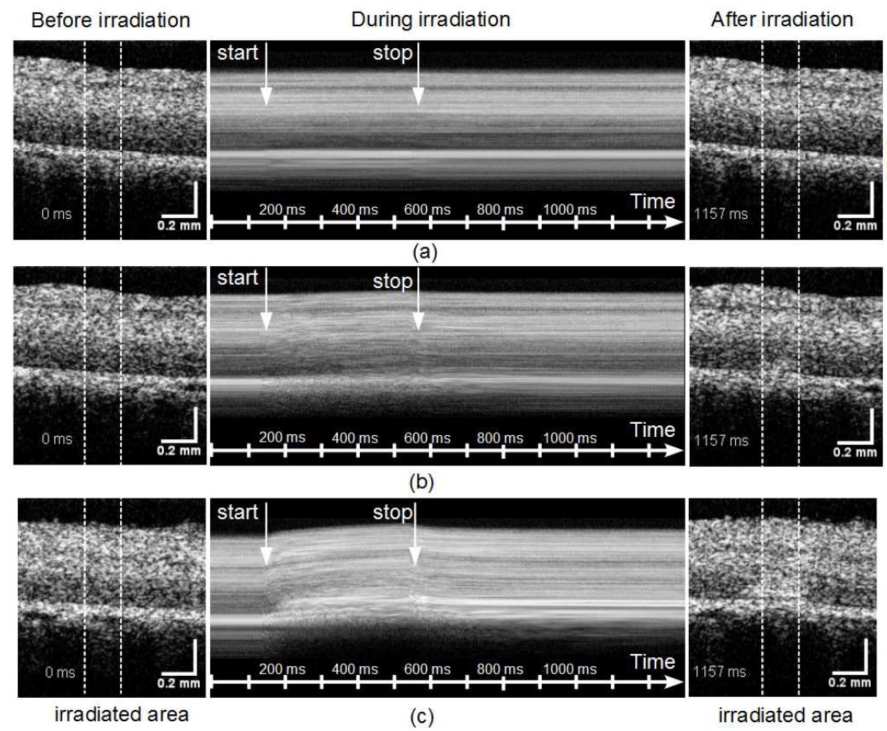

OCT images before (left) and after (right) the irradiation for three representative lesions 89W/cm$_2$ (a), 220W/cm$_2$ (b), and 400W/cm$_2$ (c).

Müller, Heike H., et al. "Imaging thermal expansion and retinal tissue changes during photocoagulation by high speed OCT." *Biomedical optics express* 3.5 (2012): 1025-1046.

Color-Doppler OCT of Photocoagulation

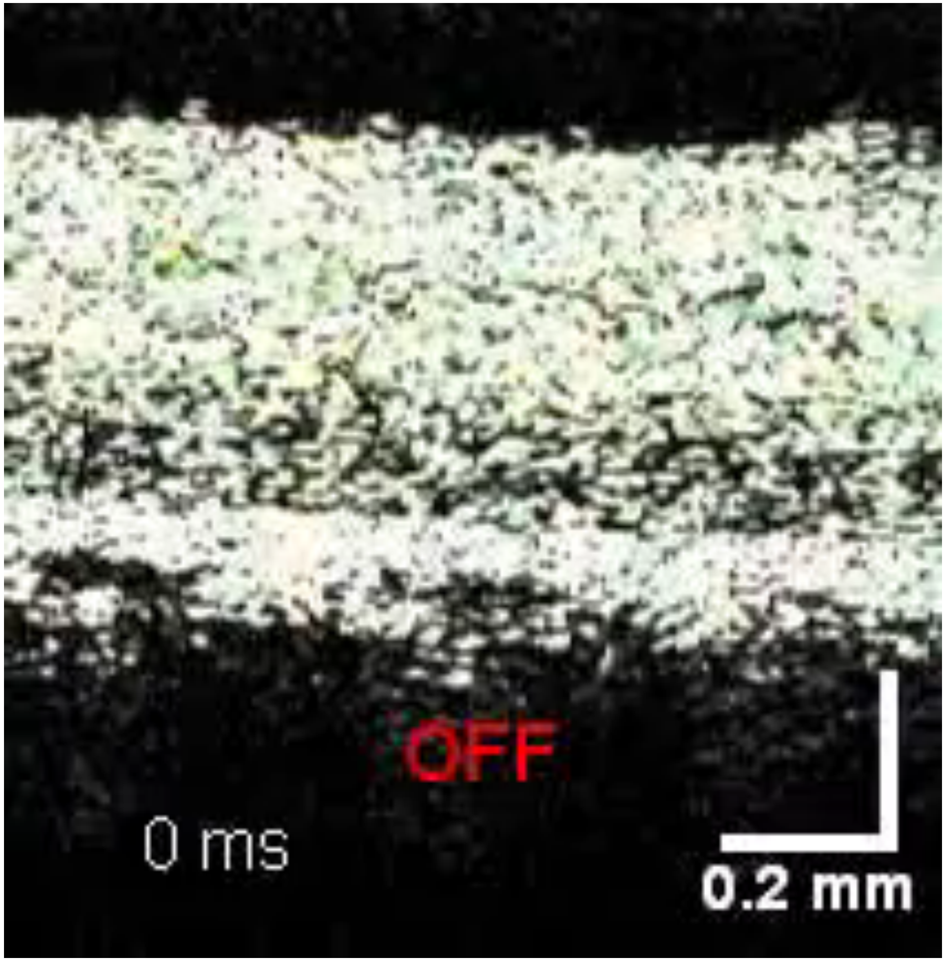

Color-Doppler OCT of Photocoagulation

89W/cm2

220W/cm2

400W/cm2

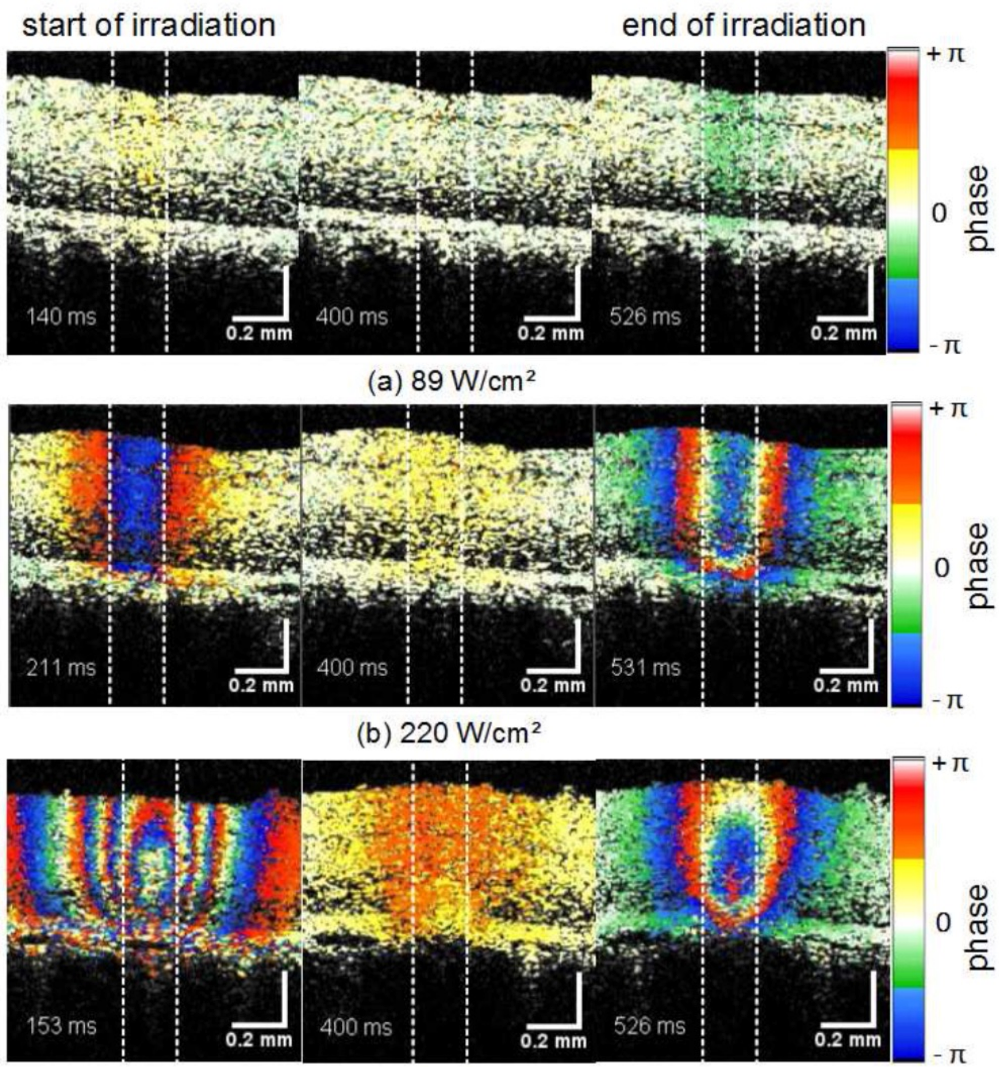

(a) 89 W/cm²

(b) 220 W/cm²

(c) 400 W/cm²

Acoustic Radiation Force Impulse (ARFI) Shear-Wave Elastography

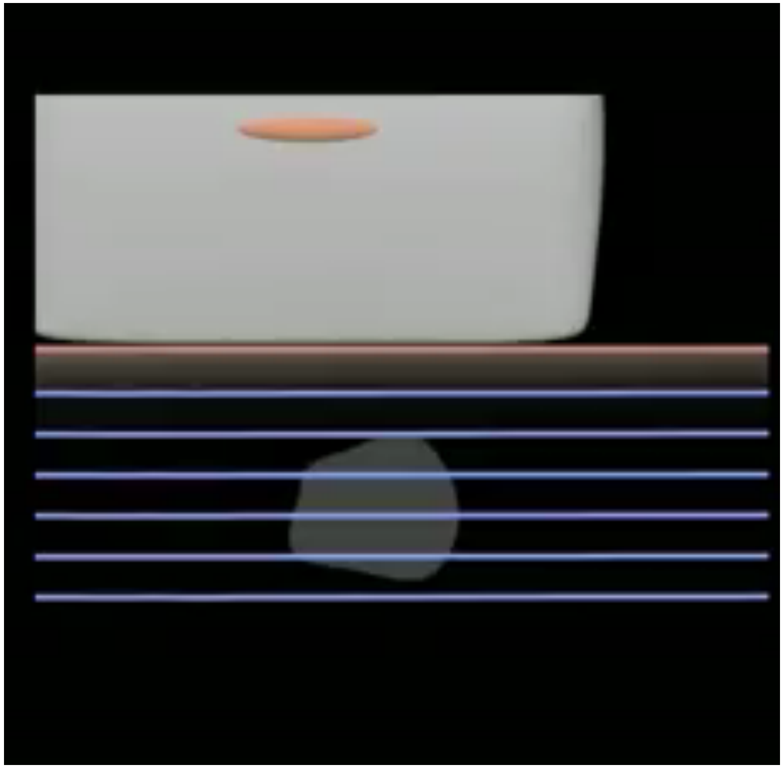

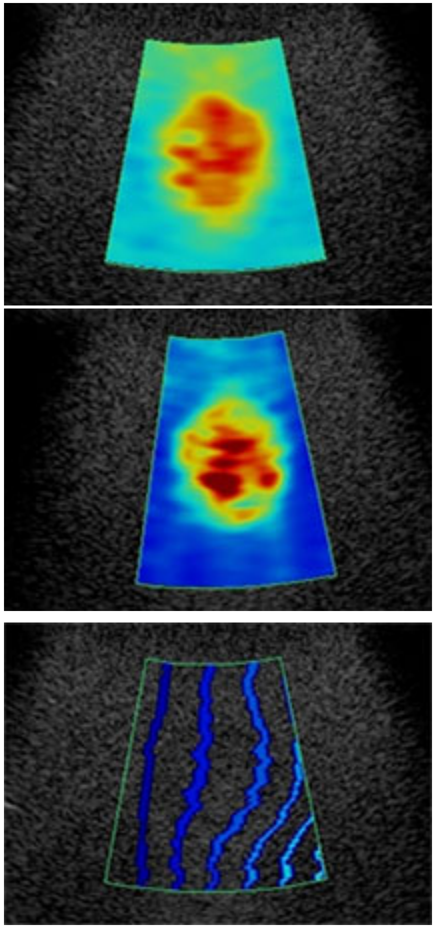

Shear wave speed (m/s)

Elasticity (kPa)

Propagation

TOSHIBA

Ultrafast Ultrasound Imaging

fultrasound

Conventional ultrasound imaging

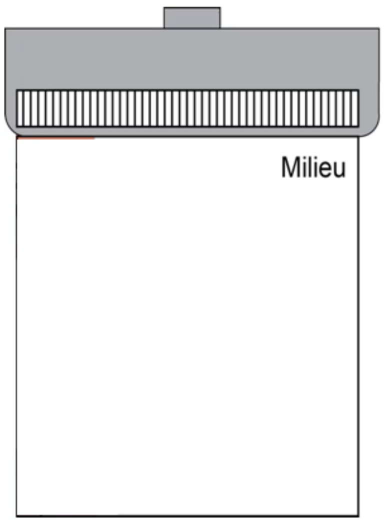

1/ Transmit focused ultrasound

Verasonics® Supersonic imagine http://fultrasound.eu/science-technology/

Imaging Feedback using Ultrasound Shear Wave Elastography

Spatial-temporal displacement images acquired after the shear wave generation in the *ex vivo* kidneys:

(a) control

(b) 100 pulses

(c) 1000 pulses

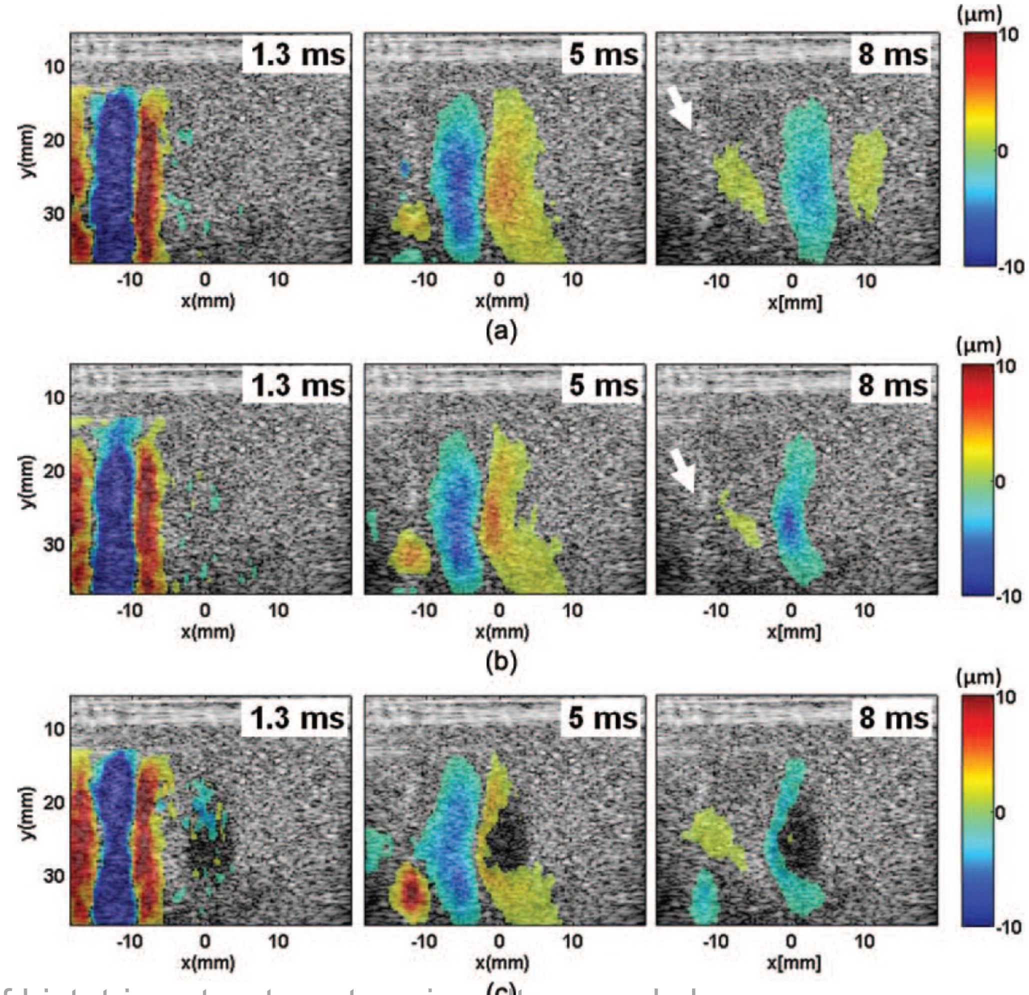

Wang, Tzu-Yin, et al. "Imaging feedback of histotripsy treatments using ultrasound shear wave elastography." *Ultrasonics, Ferroelectrics, and Frequency Control, IEEE Transactions on* 59.6 (2012): 1167-1181.

Heavy Ion UTOPIA by Tobias

- **Perform radiotherapy and image diagnosis simultaneously**

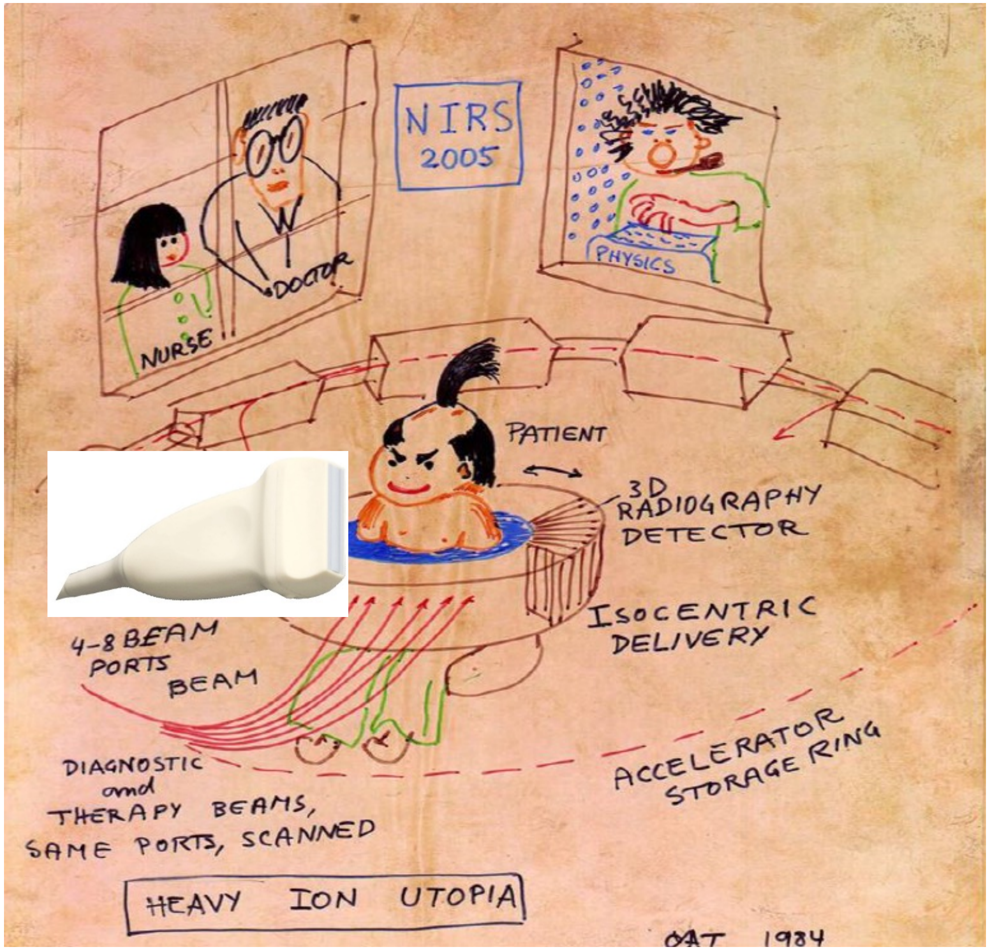

Q&A